

Singularity-Consistent Path Planning and Control of Parallel Robot Motion Through Instantaneous-Self-Motion Type Singularities

D.N. Nenchev

M. Uchiyama

Dept. of Aeronautics and Space Engineering
Tohoku University
Aramaki-aza-Aoba, Aoba-ku, Sendai 980-77, JAPAN

Abstract

We apply our newly proposed singularity-consistent path tracking approach to nonredundant parallel-link manipulators. We analyze the singularities of such mechanisms, assuming that the output-link moves on a pre-defined and parameterizable path. Especially, we focus on the so-called instantaneous self-motion type singularity. We propose a closed-loop controller that guarantees asymptotic stability when tracking paths through such a singularity. As a comprehensive analytical example we use a planar five bar mechanism. A computer simulation study is also presented, using the same example, as well as a HEXA parallel robot structure.

1. Introduction

A considerable attention in literature has been paid to analyzing singularities of serial-chain robotic mechanisms. In comparison, there is only a limited number of works that analyze singularities of parallel-chain robotic mechanisms [1], [2]-[4], [8], [12], [13]. As far as control around singularities is concerned, only a few papers are available regarding serial-link manipulators, and there is almost no discussion on this topic for parallel-link devices.

Recently we proposed a new method for path planning and control of serial link manipulators, around, and at singularities, called *singularity-consistent path tracking* [5], [6]. We have shown that while tracking paths passing through singularities of a generic robotic mechanism, it is generally possible to achieve stability, and at some specific singularities even asymptotic stability can be guaranteed. In this paper we show that it

is straightforward to apply the singularity-consistent formulation to parallel link manipulators.

The paper is organized as follows. In section 2, we derive the singularity-consistent equations for a parallel-link manipulator. Singularity analysis from the viewpoint of pre-defined path tracking capability is presented in section 3. An analytical example is shown in section 4. A closed-loop controller is proposed in section 5. Results from a computer simulation, including a planar and a spatial example, are given in section 6. Finally, a discussion and conclusion can be found in section 7.

2. Singularity-Consistent Kinematic Formulation for Parallel Robots

It is well known that the kinematic function of a parallel robot is represented as an implicit smooth vector-valued function

$$\varphi(\mathbf{p}, \Theta) = \mathbf{0}, \quad (1)$$

reflecting the physical phenomenon of a closed kinematic chain [1], [11]. In the above notation $\Theta \in \mathbb{R}^n$ denotes the coordinates of the active joints (the actuated joints), whereas $\mathbf{p} \in \mathbb{R}^n$ stands for the output-link coordinates¹.

Velocity-based control of parallel-link manipulators utilizes the following equation, obtained after differentiation of eq. (1):

$$\mathcal{D}_p \varphi(\mathbf{p}, \Theta) \dot{\mathbf{p}} + \mathcal{D}_\theta \varphi(\mathbf{p}, \Theta) \dot{\Theta} = \mathbf{0}, \quad (2)$$

where \mathcal{D} denotes the differential operator. In coordinate form, both differential mappings $\mathcal{D}_p \varphi$ and $\mathcal{D}_\theta \varphi$

¹We consider only non-redundant systems.

are represented by $n \times n$ matrices. Velocity-based control after the above equation degrades severely whenever any of the above mappings, or both, become ill-conditioned.

In this paper, we propose a new formulation of the velocity equation to avoid the above drawback. Suppose that the output-link path can be parametrized as $\mathbf{p} = \boldsymbol{\gamma}(s)$, where $\boldsymbol{\gamma} : \mathbb{R}^1 \rightarrow \mathbb{R}^n$ is a smooth function and the parameter s is not time. Then, the kinematic function is rewritten as:

$$\boldsymbol{\varphi}(\boldsymbol{\gamma}(s), \boldsymbol{\Theta}) = \mathbf{0}. \quad (3)$$

After differentiation, we obtain

$$\mathcal{D}_s \boldsymbol{\varphi}(\boldsymbol{\gamma}(s), \boldsymbol{\Theta}) \dot{s} + \mathcal{D}_{\boldsymbol{\Theta}} \boldsymbol{\varphi}(\boldsymbol{\gamma}(s), \boldsymbol{\Theta}) \dot{\boldsymbol{\Theta}} = \mathbf{0}, \quad (4)$$

where the mapping $\mathcal{D}_s \boldsymbol{\varphi} = (d_1^s \ d_2^s \ \dots \ d_n^s)^T$ is an n -dimensional vector-valued function, whereas the mapping $\mathcal{D}_{\boldsymbol{\Theta}} \boldsymbol{\varphi}$ is represented by an $n \times n$ matrix. It is apparent that with this representation, system dimension is decreased, as compared to the dimension of the “conventional” equation (2).

For convenience of notation, we augment the active-joint space by the path parameter s :

$$\mathbf{q} = (s, \boldsymbol{\Theta}^T)^T \quad (5)$$

and rewrite eq. (3) as

$$\boldsymbol{\eta}(\mathbf{q}) = \mathbf{0}, \quad (6)$$

where $\boldsymbol{\eta} : \mathbb{R}^{n+1} \rightarrow \mathbb{R}^n$ is smooth because it is composed of two smooth mappings. Let us introduce a linear local model at \mathbf{q} :

$$\mathcal{D}_q \boldsymbol{\eta}(\mathbf{q}) \dot{\mathbf{q}} = \mathbf{0}, \quad (7)$$

where the tangential space mapping $\mathcal{D}_q \boldsymbol{\eta}$ is composed of $\mathcal{D}_s \boldsymbol{\gamma}$, the gradient function for $\boldsymbol{\gamma}$, and the tangential space mapping $\mathcal{D}_{\boldsymbol{\Theta}} \boldsymbol{\varphi}$ of the kinematic function². In fact, we arrived at a homogeneous $n \times (n+1)$ -dimensional system. A set of solutions exists, that can be represented as follows:

$$\dot{\mathbf{q}} = b \boldsymbol{\nu}(\mathbf{q}), \quad (8)$$

where b is an arbitrary scalar, and $\boldsymbol{\nu} \in \mathbb{R}^{n+1}$ is the so-called *null space function* [7]. We point out that the formulation of the type (8) is easily implemented for path planning and control, as shown on our previous works [5], [6]. The arbitrary scalar b can be determined from the desired motion velocity. The system is

²When not missleading, we shall omit functional dependence.

decoupled in terms of direction of motion, represented by the null space function $\boldsymbol{\nu}$, and velocity, represented by the scalar variable b .

At this point, without a loss of generality, we shall take advantage of the fact that for a number of parallel-link mechanisms the mapping $\mathcal{D}_{\boldsymbol{\Theta}} \boldsymbol{\varphi}$ is represented in a diagonal form: $\mathcal{D}_{\boldsymbol{\Theta}} \boldsymbol{\varphi} = \text{diag}(d_{11}^{\boldsymbol{\Theta}} \ d_{22}^{\boldsymbol{\Theta}} \ \dots \ d_{nn}^{\boldsymbol{\Theta}})$. Then, the column-augmented system matrix is

$$\mathcal{D}_q \boldsymbol{\eta}(\mathbf{q}) = \begin{pmatrix} d_1^s & d_{11}^{\boldsymbol{\Theta}} & & \mathbf{0} \\ d_2^s & & d_{22}^{\boldsymbol{\Theta}} & \\ \dots & & \ddots & \\ d_n^s & \mathbf{0} & & d_{nn}^{\boldsymbol{\Theta}} \end{pmatrix},$$

whereas the null space function becomes

$$\boldsymbol{\nu}(\mathbf{q}) = (v_o \ v_1 \ \dots \ v_n)^T, \quad (9)$$

$$v_o = \prod_{i=1}^n d_{ii}^{\boldsymbol{\Theta}}, \quad v_i = -\frac{d_i^s}{d_{ii}^{\boldsymbol{\Theta}}} \prod_{j=1}^n d_{jj}^{\boldsymbol{\Theta}}, \quad i = 1, \dots, n.$$

Note that the division by $d_{ii}^{\boldsymbol{\Theta}}$ in the v_i term is used for convenience of notation only.

The above representation simplifies the singularity analysis considerably, as we shall show in the next section.

3. Singularity Analysis from the Viewpoint of Pre-Defined-Path Tracking Capability

Most studies on singularities of robotic mechanisms focus on the identification and classification of singular configurations in a general sense, without considering a specific motion path for the output link. In our recent works introducing the singularity-consistent technique for serial-link manipulators, we took a different approach, that is based on analyzing the singularity with regard to the desired end-effector path [5], [7]. This approach provides useful insight into the path tracking capability at the singularity. The analysis revealed the existence of two types of *velocity relations* at a singular point :

- Type A velocity relation, when the null space function $\boldsymbol{\nu}(\mathbf{q})$ does not vanish, and
- Type B velocity relation, when the null space function vanishes.

The importance of analyzing for the specific velocity relation is related to the path tracking capability.

In terms of control, Type A relation yields asymptotic stability, while the stability with Type B relation is generally not asymptotic, and hence, special assumptions are to be made [5]. We conclude therefore that besides a general singularity analysis, it is crucial to analyze the singularity for the specific velocity relation under the pre-defined path condition.

Next, we shall analyze the singularities of a parallel-link manipulator. Note that with regard to eq. (4), a non-singular configuration \mathbf{q} would imply the non-singularity of both matrices $\mathcal{D}_\theta \boldsymbol{\eta}(\mathbf{q})$ and $\mathcal{D}_s \boldsymbol{\eta}(\mathbf{q})$. With regard to the column-augmented system and the null space function (9), a non-singular configuration \mathbf{q} implies:

- $\forall d_{ii}^\theta(\mathbf{q}) \neq 0$ and $\exists d_i^s(\mathbf{q}) \neq 0$, $i = 1, \dots, n$.

On the other hand, a singular configuration \mathbf{q}_s is identified by either of the following four conditions:

- *instantaneous self-motion (S1)*: $\exists d_{ii}^\theta(\mathbf{q}_s) = 0$ and $v_i(\mathbf{q}_s) \neq 0$;
- *dual instantaneous self-motion (S2)*: $\forall d_{ii}^\theta(\mathbf{q}_s) \neq 0$ and $\forall d_i^s(\mathbf{q}_s) = 0$;
- *bifurcation I (S3)*: $\exists d_{ii}^\theta(\mathbf{q}_s) = 0$ and $d_i^s(\mathbf{q}_s) = 0$;
- *bifurcation II (S4)*: two or more $d_{ii}^\theta(\mathbf{q}_s) = 0$.

It is apparent that at the first two types of singularity the velocity relation is of Type A. The first singularity (S1) is an instantaneous self-motion singularity since the first element of the null space function vanishes, and the output link must pause. Note also that $v_i(\mathbf{q}_s) \neq 0$ implies $\forall d_{jj}^\theta(\mathbf{q}_s) \neq 0$, $j \neq i$ and $d_i^s(\mathbf{q}_s) \neq 0$. This is a codimension 1 singularity.

In case of the second singularity (S2), the motion of the mechanism can be considered as a special type of “self-motion”, which we call *dual instantaneous self-motion*. We propose this term, having in mind the duality in properties of serial-link and parallel-link manipulators [10], [11]. In the conventional sense, under self-motion of a (serial-link) mechanism it is understood that the end-effector is motionless while there is some motion in the joints (finite or infinite small). By dual self-motion of a parallel-link mechanism we mean just the opposite situation: the motion of the output-link does not imply any motion (finite or infinite small) in active-joint space. We note that with a specific metric, both types of instantaneous self-motion will yield finite self-motion.

The dual instantaneous self-motion singularity deserves special attention. Since the active joints must be at rest, obviously the output-link moves only due to the non-zero velocity in the passive joints. In this situation, it is essential that the actual motion of the

output-link follows strictly the parametrized trajectory in terms of position and velocity, since the motion is unobservable. Any deviation from the trajectory will result in an uncontrollable state. In practice, due to various reasons, this requirement is hardly to be met. The discussion on possible approaches to the problem goes beyond the scope of this paper.

At the third and the fourth type of singularity the null space function (9) vanishes; the velocity relation is of Type B and there is a bifurcation. Bifurcation I depends on $d_i^s(\mathbf{q}_s)$ and hence, on the output-link path. In other words, at the same kinematically singular configuration $\boldsymbol{\Theta}_s$, there will be either a Bifurcation I (Type B) velocity relation, or an instantaneous self-motion (Type A) velocity relation, depending on the specific output-link path. On the other hand, at Bifurcation II, the rank of the tangential space mapping \mathcal{D}_θ decreases by more than one. There is no dependence on the output-link path at all.

4. Analytical Example: A Five Bar Robotic Mechanism

Let us consider a five bar mechanism as in Figure 1. We regard this mechanism as a dual equivalent of a 2R planar serial-link arm, which we analyzed in [5]. Point T is the end-point, $\boldsymbol{\Theta} = (\theta_1, \theta_2)$ are the active joint coordinates, a_i , l_i and m_i denote the distance from the origin to the active joint, arm length, and rod length, respectively. Further on, we assume that the end-point has to track a straight-line path, parameterized as:

$$\mathbf{p} = s \begin{bmatrix} \cos \gamma \\ \sin \gamma \end{bmatrix} + \mathbf{p}^{init}, \quad (10)$$

where s is the path parameter, γ denotes the (constant) inclination angle of the path, and \mathbf{p}^{init} denotes the end-point coordinates at the initial position.

The i -th element of the kinematic function is derived from the geometrical relation for the i -th kinematic chain:

$$\eta_i(\mathbf{q}) \equiv \frac{1}{2} \left(\left\| \overrightarrow{\mathbf{b}_i \mathbf{p}} \right\|^2 - m_i^2 \right) = 0, \quad (11)$$

where $\mathbf{b}_i = \begin{bmatrix} (-1)^{i-1} a_i + l_i \cos \theta_i \\ l_i \sin \theta_i \end{bmatrix}$ denotes the vector from the origin to the passive joint connecting the arm and the rod.

Next, we derive the tangential space mappings $\mathcal{D}_s \boldsymbol{\eta}$ and $\mathcal{D}_\theta \boldsymbol{\eta}$:

$$\mathcal{D}_s \boldsymbol{\eta}(\mathbf{q}) \equiv \frac{\partial \boldsymbol{\eta}(\mathbf{q})}{\partial s} = \begin{bmatrix} (\mathbf{p} - \mathbf{b}_1)^T \\ (\mathbf{p} - \mathbf{b}_2)^T \end{bmatrix} \frac{\partial \mathbf{p}}{\partial s}, \quad (12)$$

and each element is

$$d_i^s(\mathbf{q}) = k_i \cos \gamma + l_i \cos(\gamma - \theta_i) - s - p_2^{init} \sin \gamma, \quad (13)$$

where $k_i = (-1)^{i-1} a_i - p_1^{init}$. On the other hand, we have

$$\mathcal{D}_\theta \boldsymbol{\eta} \equiv \frac{\partial \boldsymbol{\eta}(\mathbf{q})}{\partial \boldsymbol{\Theta}} = - \begin{bmatrix} (\mathbf{p} - \mathbf{b}_1)^T \frac{\partial \mathbf{b}_1}{\partial \theta_1} & 0 \\ 0 & (\mathbf{p} - \mathbf{b}_2)^T \frac{\partial \mathbf{b}_2}{\partial \theta_2} \end{bmatrix}, \quad (14)$$

and

$$d_{ii}^\theta(\mathbf{q}) = l_i(k_i \sin \theta_i + s \sin(\gamma - \theta_i) + p_2^{init} \cos \theta_i). \quad (15)$$

The null space function is finally obtained as

$$\boldsymbol{\nu}(\mathbf{q}) = \begin{bmatrix} d_{11}^\theta d_{22}^\theta \\ -d_1^s d_{22}^\theta \\ -d_2^s d_{11}^\theta \end{bmatrix}. \quad (16)$$

Now it can be easily verified that whenever:

- either the left or the right kinematic subchain is extended, one of the elements d_{ii}^θ is zero, yielding singularity of type (S1). The end-point must pause, since the first element of the null space function is zero. This represents self-motion in the conventional sense.
- the two links adjacent to the end-point are aligned, both elements $d_i^s, i = 1, 2$ are zero, yielding singularity of type (S2). This represents the dual instantaneous self-motion of the mechanism.
- both kinematic subchains are extended (the passive joint angles become zero), both elements $d_{ii}^\theta, i = 1, 2$ are zero, yielding singularity of type (S4). This type of singularity represents a stationary point of the nonlinear system (8). It can be easily verified that this particular singularity of the five bar mechanism represents an isolated point singularity (there are no real roots, it is not a bifurcation).

It is seen that the majority of the singularities of the five-bar parallel-link robotic mechanism are characterized with Type A velocity relation. This means that using the singularity-consistent formulation, *kinematic control with asymptotic stability would be feasible*. This will be shown in the next section.

5. Closed-Loop Controller

In designing the closed-loop controller, we shall exploit the fact that the kinematic function of the

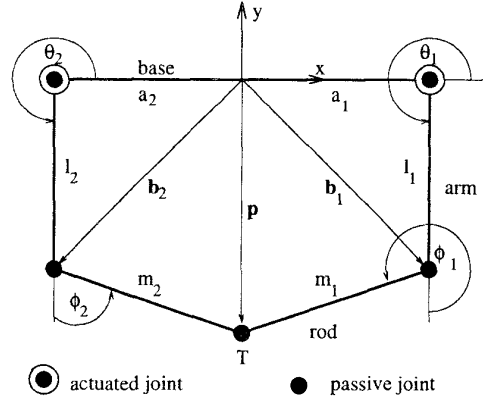


Figure 1. The five bar mechanism.

parallel-link manipulator is an implicit one, and is written as in eq. (6). We define a system error as $\mathbf{e} = \boldsymbol{\eta}(\mathbf{q})$. This error includes the path tracking error implicitly. Further on, we use the following Lyapunov function candidate:

$$v = \frac{1}{2} \mathbf{e}^T \boldsymbol{\Lambda} \mathbf{e} = \frac{1}{2} \boldsymbol{\eta}^T \boldsymbol{\Lambda} \boldsymbol{\eta}, \quad (17)$$

where $\boldsymbol{\Lambda}$ is a positive definite gain matrix. Noting that $\dot{\mathbf{e}} = (\mathcal{D}_q \boldsymbol{\eta}) \dot{\mathbf{q}}$, and substituting into the derivative of the Lyapunov function, we obtain

$$\dot{v} = \boldsymbol{\eta}^T \boldsymbol{\Lambda}^T (\mathcal{D}_q \boldsymbol{\eta}) \dot{\mathbf{q}}. \quad (18)$$

Next, let

$$\dot{\mathbf{q}} = -(\mathcal{D}_q \boldsymbol{\eta})^+ \boldsymbol{\Lambda} \boldsymbol{\eta} \pm b \boldsymbol{\nu}(\mathbf{q}), \quad (19)$$

where $(\cdot)^+$ denotes the pseudoinverse. With this choice of $\dot{\mathbf{q}}$, and a nonsingular matrix $\mathcal{D}_q \boldsymbol{\eta}$, the system will be asymptotically stable because of the negativity of the derivative (18). We note that a nonsingular matrix $\mathcal{D}_q \boldsymbol{\eta}$ implies a regular point or an instantaneous self-motion type singularity.

The structure of this closed-loop controller is depicted in Figure 2.

6. Computer Simulation

We shall examine the performance of the proposed technique through computer simulation, using the five bar robotic mechanism from the analytical example, as well as a model of the HEXA parallel robot [8], [9]. In both cases, the closed-loop controller from the previous section is applied.

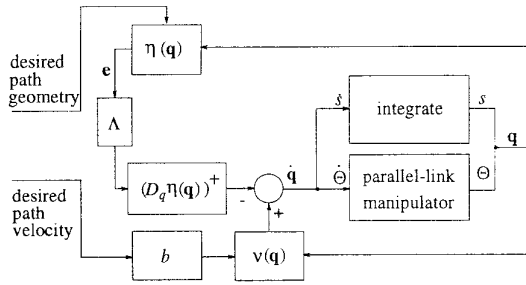


Figure 2. The closed-loop controller.

6.1. The Five Bar Robotic Mechanism

The geometry of the mechanism is: $l_i = a_i = 1$ m, $m_i = 1.12$ m. The initial configuration has been defined by $\theta_i^{init} = -\frac{\pi}{2}$ rad, $p_1^{init} = 0$ m, $p_2^{init} = -1.5$ m. The desired path is a straight-line segment with constant slope angle $\gamma = \frac{3\pi}{4}$ rad. In the augmented joint space, this path induces a manifold represented by a closed-curve, as already pointed out. Figure 3 visualizes this curve mapped onto the active-joint space and onto the passive-joint space.

The desired path velocity is specified by a constant $b = 1$. In this case, the velocity of the end-point is obtained “naturally”, from the curvature of the straight-line-path-induced manifold in augmented joint space. The duration is set to 14 s, which results in a full-cycle motion. The straight-path segment is traversed several times (see Figure 4). The mechanism moves through both types of instantaneous self-motion singularities³, including the dual instantaneous self-motion singularity (2). This demonstrates the fact that the algorithm does not deteriorate, and delivers a proper active-joint velocity solution. Motion “through” the instantaneous self-motion singularities (1) is possible, since the end-point velocity becomes zero, whereas the active- and the passive-joint velocity of the extended chain are nonzero. At those singularities the end-point reverses the direction. On the other hand, motion “through” the dual instantaneous self-motion singularities (2) might be possible⁴, since both active-joint velocities are zero, whereas the end-point velocity and the two passive-joint velocities are continuous. The two system errors as defined in the previous section, are depicted in Figure 5.

³The type of the singularity is indicated with numbers.

⁴Study on the dynamics of motion is necessary to clarify this possibility.

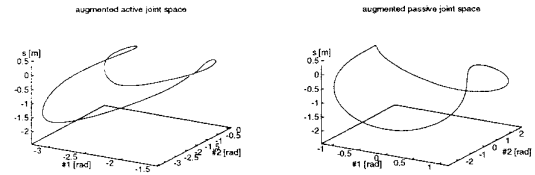


Figure 3. Closed-curve mappings of the straight-line path.

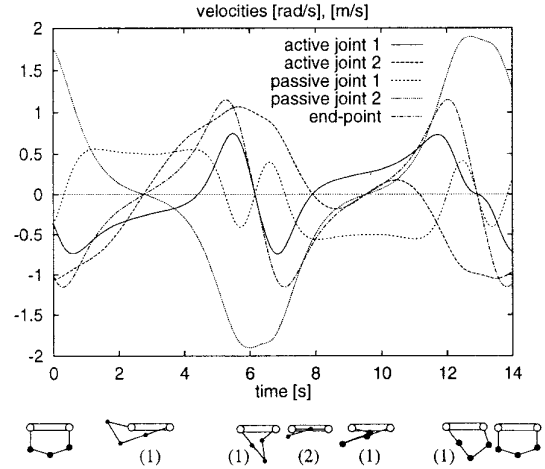


Figure 4. Motion along a straight-line path with 135 deg inclination.

6.2. The HEXA Parallel-Link Robot

The HEXA robot has been studied in our recent works [8], [9], where the reader can find the main geometrical and kinematical parameters. This is a very fast six DOF parallel-link robot (Figure 6). We ap-

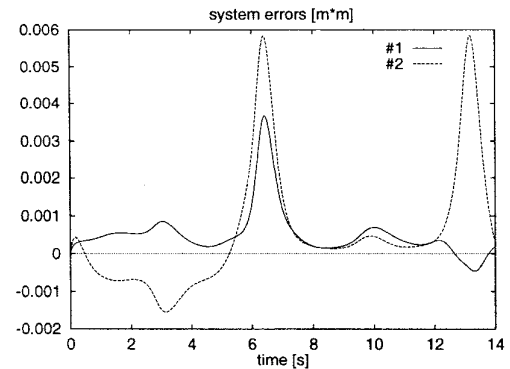


Figure 5. System errors.

ply the technique suggested in this paper to the robot. The desired output-link path is specified as a straight-line. The initial position of the output-link is selected as -0.704 m along the vertical axis, while the orientation is $+0.128$ rad around that axis. This initial configuration has been chosen to guarantee robot motion only through instantaneous self-motion type singularities, while the output link moves along a path parallel to the horizontal x axis. The duration of the motion is 10 s. Basically, the motion is performed with constant scaling factor $b = 3 \times 10^6$. This value was determined experimentally in order to obtain realistic joint velocities. Only during the initial/final 2 s of the motion, we use a fifth order polynomial for b in order to guarantee smooth acceleration/deceleration.

Simulation results are shown in Figure 7. It is seen that while the path parameter s is at its maximum, the diagonal element d_{66}^{θ} moves through zero, indicating an instantaneous self-motion type singularity. Around this singularity, the output-link is obviously at rest (constant s). Motion continues smoothly, while the output-link reverses direction. Later on, the robot enters another singularity of the same type, with re-configuration of the second kinematic chain (d_{22}^{θ} goes through zero). The (active) joint angles and velocities are also displayed in the figure. It is interesting to note that motion “through” each singularity is done by using only one of the motors.

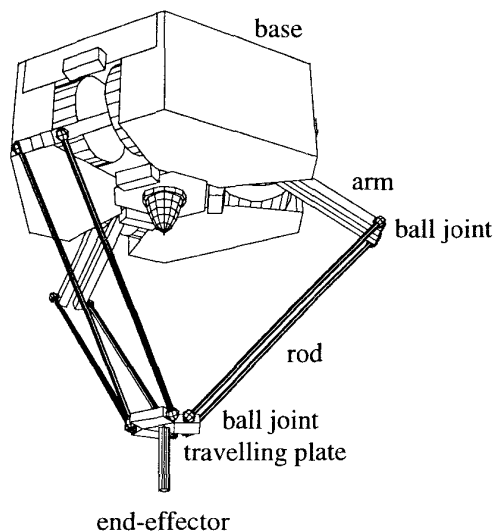


Figure 6. The HEXA parallel-link robot.

7. Conclusion and Discussion

In this paper, the newly proposed singularity-consistent path tracking approach has been applied to nonredundant parallel-link manipulators. We analyzed the singularities of such mechanisms, based on the new formulation. Especially, we focused on the instantaneous self-motion type singularity. A controller has been proposed, that guarantees asymptotic stability when tracking paths through such a singularity. As a comprehensive analytical example we used the planar five bar mechanism. The same example was studied with computer simulation. The theoretical results have been confirmed through another simulation using the HEXA parallel robot structure. Meanwhile, successful experimental verification has been done with HEXA. The results will be reported elsewhere. We note that computational requirements are not demanding, since the null space function is easily calculated.

In this work we have also shown that theoretically it is possible to move through the dual instantaneous self-motion singularity as well. In order to evaluate the feasibility for practical implementation, study on the motor-torque requirement is necessary. Finally, further study on the bifurcation-type singularities is needed, both from a theoretical and from a practical viewpoint.

References

- [1] C. Gosselin and J. Angeles, “Singularity analysis of closed loop kinematic chains,” *IEEE Trans. Robotics and Automation*, Vol. 6, No. 3, pp. 281–290, June 1990.
- [2] S. Lee and S. Kim, “Kinematic feature analysis of parallel manipulator systems,” in *Proc. 1994 IEEE Int. Conf. Robotics and Automation*, San Diego, California, May 1994, pp. 77–82.
- [3] O. Ma and J. Angeles, “Architecture singularities of platform manipulators,” in *Proc. 1991 IEEE Int. Conf. Robotics and Automation*, Sacramento, California, April 9–11, 1991, pp. 1542–1547.
- [4] J.P. Merlet, “Singular configurations of parallel manipulators and Grassman geometry,” *The Int. Journal of Robotics Research*, Vol. 8, No. 5, pp. 45–56, 1989.
- [5] D.N. Nenchev and M. Uchiyama, “Singularity consistent path tracking: a null-space based approach,” in *Proc. 1995 IEEE Int. Conf. Robotics and Automation*, Nagoya, Japan, May 21–27, 1995, pp. 2482–2489.

- [6] D.N. Nenchev, "Tracking manipulator trajectories with ordinary singularities: a null space based approach," *The Int. J. of Robotics Research*, Vol. 14, No. 4, pp. 399-404, 1995.
- [7] D.N. Nenchev and M. Uchiyama, "Singularity consistent velocity command generation for nonredundant robots," in *Proc. 1995 Int. Conf. on Advanced Robotics (ICAR)*, Sant Feliu de Guixols, Spain, Sept. 20-22, 1995, pp. 71-78.
- [8] F. Pierrot, M. Uchiyama, P. Dauchez and A. Fournier, "A new design of a 6-DOF parallel robot," *Journal of Robotics and Mechatronics*, Vol. 2, No. 4, pp. 92-99, 1989.
- [9] M. Uchiyama, K. Iimura, F. Pierrot, P. Dauchez, K. Unno and O. Toyama, "A new design of a very fast 6-DOF parallel robot," in *Proc. 23rd Int. Symposium on Industrial Robots (ISIR)*, Barcelona, Spain, Oct. 6-9, 1992, pp. 771-776.
- [10] K.J. Waldron and K.H. Hunt, "Series-parallel dualities in actively coordinated mechanisms," in *Robotics Research: The Fourth International Symposium*, ed. by R. Bolles and B. Roth, The MIT Press, 1988, pp. 175-181.
- [11] V.B. Zamanov and Z.M. Sotirov, "Duality in mechanical properties of sequential and parallel manipulators," in *Proc. 20th Int. Symposium on Industrial Robots (ISIR)*, Tokyo, Japan, Oct. 4-6, 1989, pp. 1041-1050.
- [12] D. Zlatanov, R.G. Fenton, and B. Benhabib, "Singularity analysis of mechanisms and robots via a motion-space model of the instantaneous kinematics," in *Proc. 1994 IEEE Int. Conf. on Robotics and Automation*, San Diego, California, May 1994, pp. 980-985.
- [13] D. Zlatanov, R.G. Fenton, and B. Benhabib, "Singularity analysis of mechanisms and robots via a velocity-equation model of the instantaneous kinematics," in *Proc. 1994 IEEE Int. Conf. Robotics and Automation*, San Diego, California, May 1994, pp. 986-991.

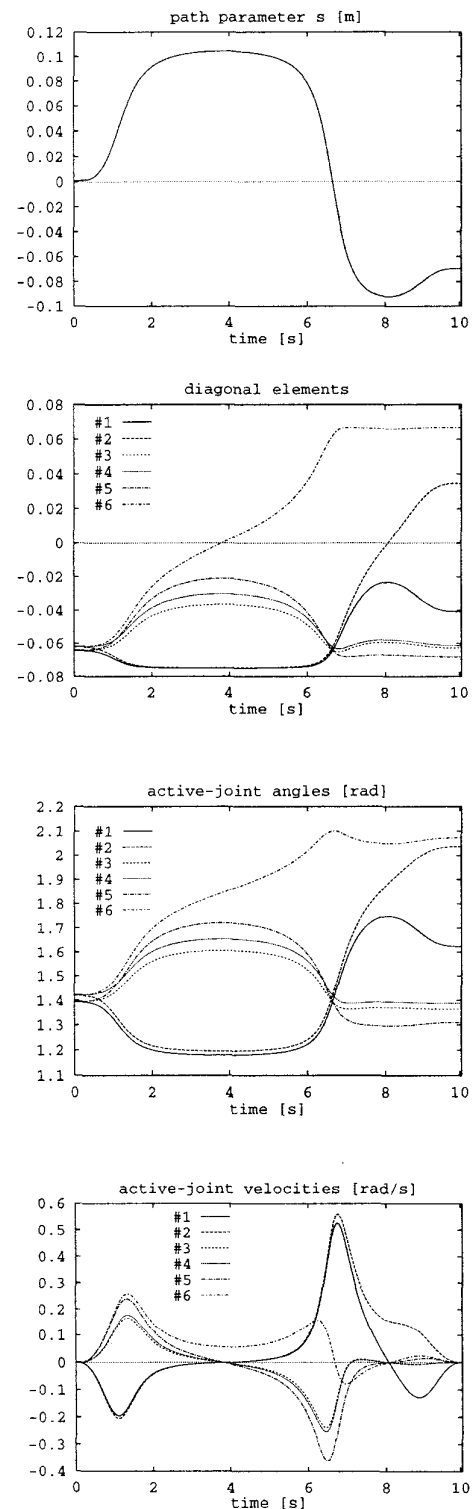


Figure 7. HEXA simulation results.